DIFFRACTION AND VECTOR MESON PRODUCTION AT HERA

MIKHAIL KAPISHIN
(for the H1 and ZEUS Collaborations)

Joint Institute for Nuclear Research, Dubna, Russia
e-mail address: kapishin@mail.desy.de

Results of new measurements of diffractive cross sections in deep-inelastic scattering (DIS) and photo-production at HERA are presented. The cross sections of dijet and open charm production are compared with next-to-leading order (NLO) QCD predictions based on parton distribution functions obtained from diffractive inclusive DIS data. A combined NLO QCD fit to the inclusive and dijet DIS data is performed to determine diffractive quark singlet and gluon densities with a better precision. Recent measurements of elastic vector meson production and deeply virtual Compton scattering at HERA are also reviewed.

1. Introduction: Hard diffraction at HERA

Diffractive processes in deep-inelastic ep scattering (DIS) and photo-production at HERA are identified by the presence of a large rapidity gap between the leading proton (or the proton dissociation system Y) and the rest of the hadronic final state X (Fig. 1)

When the hadronic final state X includes dijets and open charm, p_T of jets and mass of the charm quark provide hard scales and permit the application of perturbative QCD to the data. Within the QCD framework, the diffractive events can be interpreted as processes in which a colour singlet combination of partons is exchanged.

The variables $x_{I\!P}$ and $z_{I\!P}$ in Fig. 1 are the momentum fraction of proton carried by colour singlet exchange and the momentum fraction of colour singlet carried by
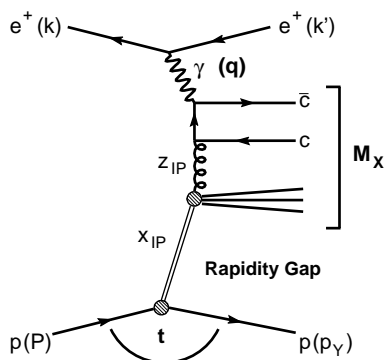
Fig. 1. The diffractive process of open charm production at HERA.

parton (quark or gluon) entering hard sub-process, respectively. t is the squared four-momentum transfer at the proton vertex.

The structure of the colour singlet can be studied using a QCD approach based on the hard scattering collinear factorization theorem [1]. It states that at fixed $x_{I\!P}$ and t, the diffractive cross section is a product of diffractive proton parton distribution functions f_i^D and partonic hard scattering cross sections $\sigma^{\gamma^* i}$

$$\sigma_r^{D(4)} \sim \sum \sigma^{\gamma^* i}(x, Q^2) \otimes f_i^D(x, Q^2, x_{I\!P}, t). \tag{1}$$

f_i^D are universal for diffractive ep DIS processes (inclusive, dijet and charm production) and obey the DGLAP evolution equations. $\sigma^{\gamma^* i}$ are the same as for inclusive DIS. This approach allows us to test the diffractive exchange within the perturbative QCD framework and extract diffractive parton distribution functions (DPDFs). The DPDFs can be applied to the analysis of boson-gluon fusion processes of dijet and charm production. These processes are directly sensitive to the gluon density in the colour singlet.

2. Measurements of inclusive diffractive DIS

High statistic samples of diffractive DIS events are selected at HERA either by requesting a large rapidity gap (LRG) in the outgoing proton direction [2, 3] or by a subtraction method differentially in the mass of the X system (the M_X method) [4]. The process measured by H1 (ZEUS) is $ep \rightarrow eXY$, where Y corresponds to any baryonic system with mass $M_Y < 1.6$ GeV ($M_Y < 2.3$ GeV). The measurements are performed in the kinematic range $2.2 < Q^2 < 1600$ GeV^2, $x_{I\!P} < 0.05$ and $|t| < 1$ GeV^2.

Both experiments have also used Forward Proton Spectrometers (FPS) to detect and measure the four-momentum of the outgoing proton in the process $ep \rightarrow eXp$ [5, 6]. This selection method has the advantages that the proton unambiguously

scatters elastically and that the squared four-momentum transfer at the proton vertex t can be reconstructed. However, the available statistics are limited by the FPS acceptance.

Together, the FPS and LRG data provide a means of studying inclusive diffraction as a function of all relevant kinematic variables. In addition to t and the usual DIS variables x and Q^2, measurements are made as a function of the fractional proton longitudinal momentum loss $x_{I\!P}$ and of $\beta = x/x_{I\!P}$, which corresponds to the fraction of the exchanged longitudinal momentum which is carried by the quark coupling to the virtual photon.

3. Dependence on $x_{I\!P}$ and t: the diffractive flux factor

The t dependence of diffractive cross sections is commonly parameterised with an exponential, $d\sigma/dt \propto e^{Bt}$. The values of B resulting from such fits to the FPS data are shown as a function of $x_{I\!P}$ in Fig. 2. At low $x_{I\!P}$, the H1 data are compatible with a constant slope parameter, $B \simeq 6$ GeV^{-2}. In a Regge approach with a single linear exchanged pomeron trajectory, $\alpha_{I\!P}(t) = \alpha_{I\!P}(0) + \alpha'_{I\!P}t$, the slope parameter B decreases with increasing $x_{I\!P}$ according to $B = B_0 - 2\alpha'_{I\!P}\ln x_{I\!P}$.
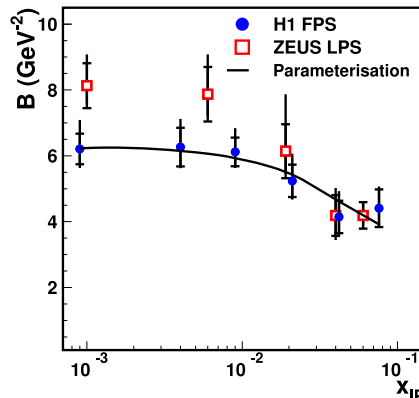

Fig. 2. Measurements of the slope parameter B by H1 and ZEUS and a parameterisation of the H1 data as used to describe the pomeron flux factor.

The low $x_{I\!P}$ H1 data thus favour a small value of $\alpha'_{I\!P} \simeq 0.06$ GeV^{-2}, though $\alpha'_{I\!P} \simeq 0.25$ GeV^{-2}, as obtained from soft hadronic interactions [7], cannot be excluded. The Regge fit to the ZEUS FPS data gives similar values for the pomeron exchange: $B_0 \simeq 7$ GeV^{-2} and $\alpha'_{I\!P} \simeq -0.03$ GeV^{-2} [3].

The $x_{I\!P}$ dependence measured by the H1 and ZEUS experiments is interpreted in terms of an effective pomeron intercept. The two results are consistent, the value of $\alpha_{I\!P}(0) = 1.118 \pm 0.008$ (exp.) $^{+0.029}_{-0.010}$ (model) coming from the H1 LRG data and $\alpha_{I\!P}(0) = 1.117 \pm 0.005$ (exp.) $^{+0.024}_{-0.007}$ (model) from the ZEUS FPS data. The

extracted $\alpha_{I\!P}(0)$ is slightly higher than the 'soft pomeron' value of $\alpha_{I\!P}(0) \simeq 1.085$, from long distance hadronic interactions [7].

The values of both $\alpha_{I\!P}(0)$ and $\alpha'_{I\!P}$ describing diffractive DIS are compatible with the results obtained for soft exclusive photo-production of ρ^0 mesons [8]. This similarity supports the picture of diffractive DIS as probing the structure of a 'soft' pomeron. 'Hard' perturbative 2-gluon exchange contributions are likely to be small.

Further analysis in which either the slope B or the intercept $\alpha_{I\!P}(0)$ is allowed to vary as a function of β and Q^2 shows no significant dependence. The $\alpha_{I\!P}(0)$ measured by ZEUS as a function of Q^2 is shown in Fig. 3. This contrasts with the Q^2 dependent effective pomeron intercept extracted in a Regge approach to inclusive low x proton structure function data, as studied in detail via the ratio of diffractive to inclusive cross sections in Ref. [2].
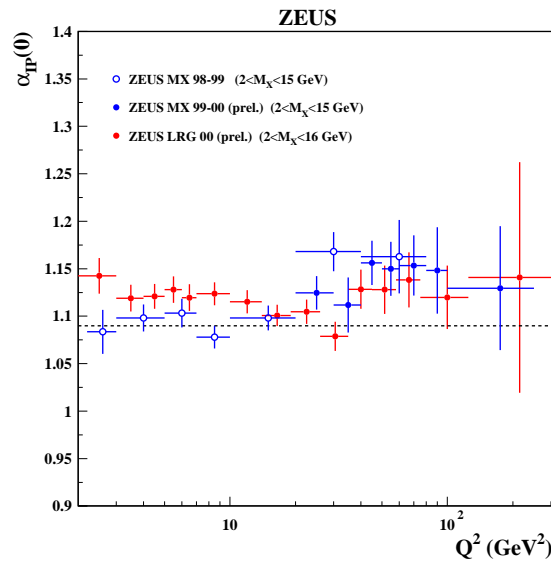

Fig. 3. The pomeron intercept $\alpha_{I\!P}(0)$ measured by ZEUS as a function of Q^2.

In general, the inclusive diffractive data are consistent with 'proton vertex' factorization [9], whereby the dependence on the variables $x_{I\!P}$, t and M_Y describing the proton vertex is completely independent of the variables β and Q^2, which describe the hard interaction with the photon. The dependence on $x_{I\!P}$ and t can then be expressed in terms of an 'effective pomeron flux' of colourless exchange, whilst the β and Q^2 dependences can be interpreted in terms of DPDFs, which describe the partonic structure of that exchange [1].

4. Dependence on $\boldsymbol{\beta}$ and $\boldsymbol{Q^2}$: diffractive parton densities

In Ref. [2], the cross section is measured differentially in β, Q^2 and $x_{I\!P}$. This is illustrated in Fig. 4. The β and Q^2 dependences of the data are interpreted in
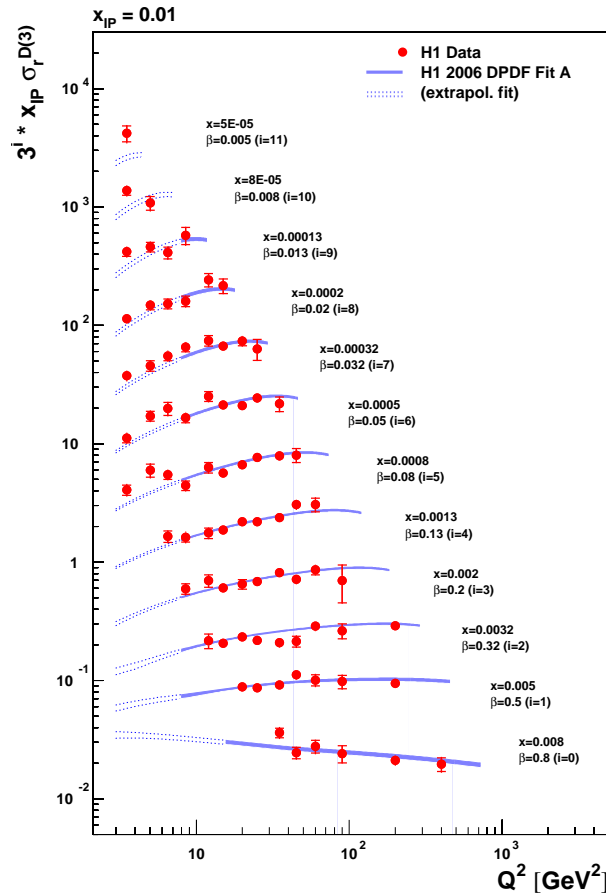
Fig. 4. The Q^2 dependence of the diffractive reduced cross section at fixed $x_{I\!P}$ and β.

a NLO DGLAP QCD fit [2] in order to extract quark singlet and gluon DPDFs. The proton vertex factorization is assumed in the QCD analysis, i.e. that the shape of DPDFs is independent on $x_{I\!P}$ and t [9]. The results are shown in Fig. 5. For the first time, the experimental and theoretical uncertainties are evaluated for diffractive parton densities. The quark singlet density is very closely related to the measured diffractive cross section and is thus well constrained, with a typical error of 5%. According to the DGLAP evolution equations, the $\ln Q^2$ derivative contains contributions due to the splittings $g \rightarrow q\bar{q}$ and $q \rightarrow qg$, convoluted with the diffractive gluon and quark densities, respectively. The derivative is determined almost entirely by the diffractive gluon density up to $\beta \simeq 0.3$. The large positive $\ln Q^2$ derivatives in this region can thus be attributed to a large gluonic component in the DPDFs. For $\beta \gtrsim 0.3$, the contribution to the Q^2 evolution from quark splittings $q \rightarrow qg$ becomes increasingly important and the derivatives become less sensitive to the gluon density. The difference between the H1 2006 DPDF fit A and fit B illustrates the uncertainty of the gluon density extracted from inclusive diffractive DIS.
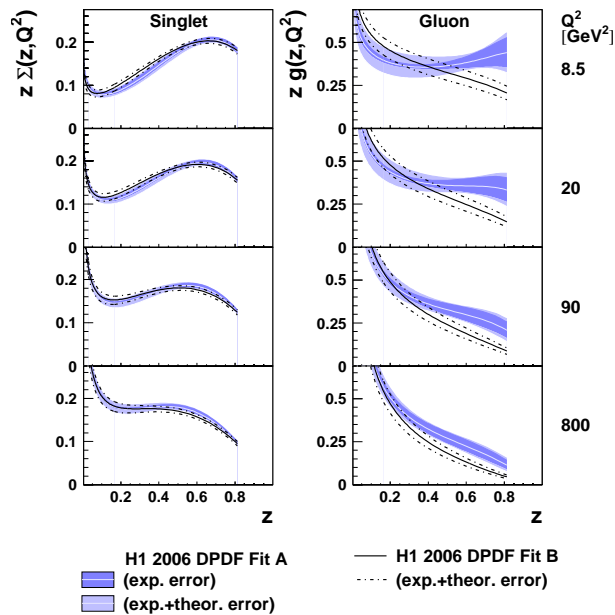
Fig. 5. *Diffractive quark singlet and gluon densities extracted from the NLO QCD H1 2006 DPDF fit A and B as functions of the parton momentum fraction z.*

These DPDFs provide important input to final state measurements such as those involving jets and charm [11, 10, 12, 13], which may also provide important additional constraints on the gluon at high β.

Integrated over β, the gluon density carries around 70% of the total momentum. A similar fraction of the total proton momentum is carried by the inclusive gluon density in the low x region where valence quark effects are small. This similarity of the ratio of quarks to gluons in the DPDFs and the inclusive proton parton densities is reflected in a ratio of the two cross sections which, to good approximation, is flat as a function of Q^2 at fixed x and $x_{I\!P}$ [2].

5. QCD analysis of $\boldsymbol{F_2^D}$ and dijet data in DIS

The dijet events are identified using the inclusive k_T cluster algorithm in the $\gamma^* - p$ rest frame. Figure 6 shows the differential dijet cross sections of H1 and ZEUS compared to NLO predictions based on DPDFs extracted from QCD fits to an inclusive diffractive structure function F_2^D [2]. The dominating process for dijet production in DIS is boson-gluon fusion. The distribution of the dijet cross section on $z_{I\!P}$ is the most sensitive to the gluon DPDF. While the prediction based on the H1 2006 DPDF fit A overestimates the dijet cross section, there is reasonable agreement between the dijet data and the H1 2006 DPDF fit B [11, 12].

The statistics of diffractive dijet events measured by H1 in DIS are sufficient to make a combined QCD fit to the inclusive diffractive and dijet data and extract one set of NLO DPDFs for quark singlet and gluon. The dijet cross sections differential in $z_{I\!P}$ and hard scale variable $p_T^2 + Q^2$ are used in the fit to constrain the gluon density.
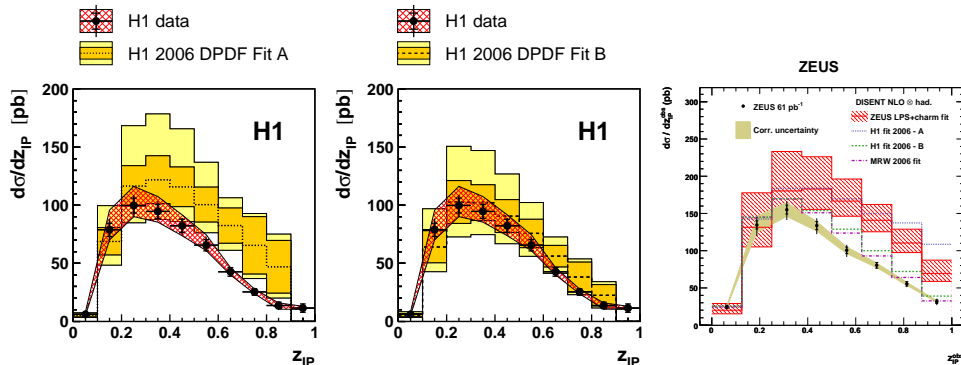
Fig. 6. *Differential cross section for diffractive dijet production in DIS as a function of $z_{I\!P}$ compared to NLO predictions based on different sets of DPDFs.*
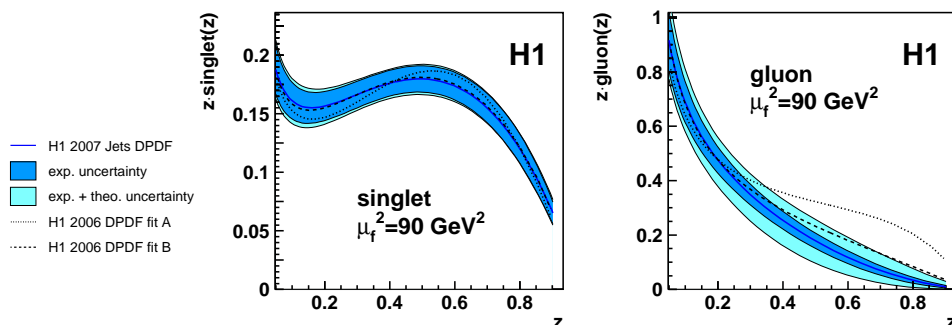

Fig. 7. *Diffractive quark singlet and gluon densities for a value of the hard scale of 90 GeV^2. The solid line indicates the combined fit, the dashed lines show the parton densities from the H1 2006 DPDF fit A and B.*

The resulting parton distributions are shown in Fig. 7. The gluon density from the combined fit is close to the result of the H1 2006 DPDF fit B. The NLO QCD DGLAP fit allows to describe both the F_2^D and the dijet cross sections with the overall value $\chi^2/ndf = 0.89$. The combined F_2^D and dijet DIS data constrain both the diffractive gluon and quark singlet densities in the fractional momentum range $0.1 < z < 0.9$. The dijet data provide big improvement in precision of the gluon density at high fractional momentum.

6. Diffractive dijets in photo-production

In dijet photo-production, the hard scale is defined by p_T of jets because $Q^2 \sim 0$. QCD collinear factorization is expected to be valid in direct processes with point-like photon, but broken in processes with resolved photon, where secondary interactions between photon and proton remnants fill rapidity gap [14]. The two processes can be separated using a variable x_γ, which corresponds to the longitudinal mo-

mentum fraction of the photon entering the hard sub-process. Resolved photon processes correspond to $x_\gamma < 1$, whereas direct photon processes to $x_\gamma \simeq 1$.
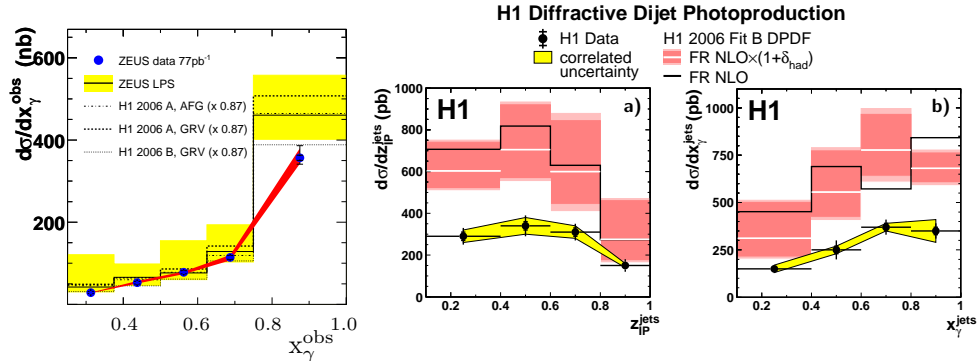

Fig. 8. *Differential cross sections of diffractive dijet photo-production compared with NLO predictions based on DPDFs extracted from inclusive diffractive DIS.*

Figure 8 shows the dijet photo-production cross section of ZEUS (left) and H1 (right) compared to the NLO calculations. Neither H1 [15], nor ZEUS [16] observe a significant difference between the quality of the description of the data in the resolved (low x_γ) and direct (high x_γ) regions by NLO predictions based on QCD collinear factorization and DPDFs [2]. However, the magnitude of the suppression of the data relative to the NLO calculations differs between the two experiments. Whilst ZEUS reports only a weak suppression of 0.8, H1 obtains a suppression by a factor of 0.5. These issues require clarification before conclusions can be drawn. Additional studies are also needed to understand the "suppression" of dijet direct photo-production [17].

7. Diffractive charm in DIS and photo-production

If QCD collinear factorization is valid, calculations based on DPDFs extracted from F_2^D should be capable to predict diffractive open charm production in shape and normalization.

The charm quark is tagged by the reconstruction of a $D^{*\pm}$ meson (H1 and ZEUS) or using the complementary measurement of a track displaced from the primary vertex (H1). The hard scale in these processes is provided by mass of the charm quark. The dominating process is the direct charm production via boson-gluon fusion and is sensitive to the gluon DPDF at low and medium fractional momentum.

The D^* DIS and photo-production data measured by H1 [10] and ZEUS [13] are found to be consistent with the NLO calculations based on DPDFs extracted from the QCD fit to inclusive diffractive DIS [2, 6]. The diffractive open charm cross sections measured by H1 and ZEUS in DIS and photo-production are shown

in Fig. 9. Within the scale uncertainties, there is no evidence for breaking of QCD collinear factorization for open charm production in DIS and γp.
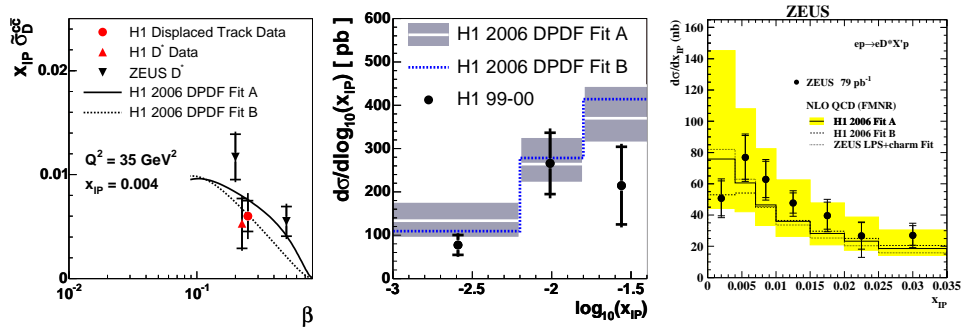

Fig. 9. Reduced cross section for open charm in DIS as a function of β (left). Differential cross section for diffractive D^* photo-production measured by H1 (middle) and ZEUS (right) as a function of $x_{I\!P}$. The data are compared with NLO DPDF predictions.

8. Exclusive vector meson production and deeply virtual Compton scattering

High-energy exclusive vector meson production in DIS is described in perturbative QCD (pQCD) through the two-gluon exchange once the scale, the virtuality of the exchanged photon Q^2, is large enough [18]. From the other side, exclusive vector meson photo-production can be used to study the effect of the vector meson mass as a hard scale. This process can be described within the framework of Regge phenomenology and the effective pomeron trajectory $\alpha_{I\!P} = \alpha_{I\!P}(0) + \alpha'_{I\!P}t$ can be extracted from the cross section dependence on the $\gamma - p$ center of mass energy, W, and t.

In this framework, the W and t dependence of the cross section can be parametrised as $\sigma(W) \propto W^\delta$ and $d\sigma/dt \propto e^{Bt}$, where t-slope B shows the transverse size of the interaction. The intercept of the pomeron trajectory $\alpha_{I\!P}(0) \simeq 1.095$ extracted from elastic ρ meson photo-production cross sections [8] is consistent with that derived from the soft hadron-hadron interactions [7]. Surprisingly, the slope $\alpha'_{I\!P} \simeq 0.12$ GeV^{-2} is found to be smaller by a factor of two than that from Ref. [7].

A steeper rise of the cross section with W is observed for heavy vector mesons $(J/\psi, \Upsilon)$ [19] compared to light vector mesons (ρ, ϕ) indicating the transition from a soft process to a hard one. A similar steeper rise of the cross section with W is seen for all vector mesons and deeply virtual Compton scattering (DVCS) $\gamma^* p \rightarrow \gamma p$, when Q^2 increases [20]. The logarithmic derivative in W increases with $Q^2 + M^2$ as

shown in Fig. 10 (left). The t-slope decreases from $B \simeq 10 \text{GeV}^{-2}$ to $B \simeq 5 \text{GeV}^{-2}$ with increasing of scale $Q^2 + M^2$ as expected in pQCD (Fig. 10, right).

DVCS process allows more direct tests of pQCD because it is free from uncertainties introduced by the vector meson wave functions. The W and t dependence of the DVCS cross section [21, 22] is in general agreement with the cross section dependence of heavy vector mesons (Fig. 10). The Q^2 dependence of the DVCS cross section is interpreted by H1 within a pQCD model [23] based on generalised parton distributions (GPDs) [24]. To describe the DVCS cross sections, the skewing effect between two involved partons is found to be large as expected in GPD models.
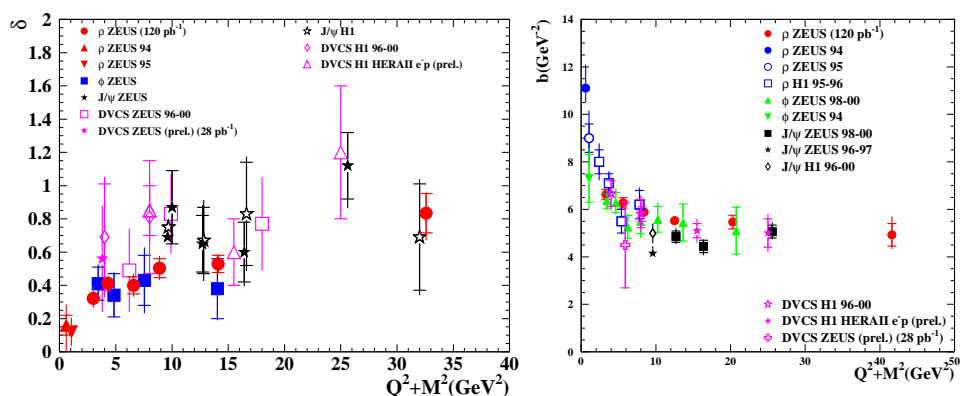

Fig. 10. A compilation of δ from $\sigma \propto W^{\delta}$ for processes of vector meson production and DVCS as a function of $Q^2 + M^2$ (left). A compilation of the t-slope B for processes of vector meson production and DVCS as a function of $Q^2 + M^2$ (right).
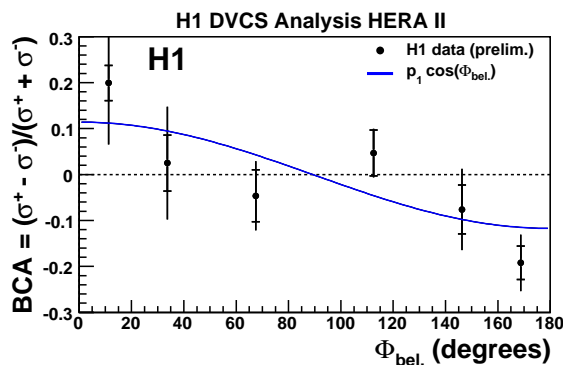

Fig. 11. Beam charge asymmetry as a function of the azimuthal angle Φ. The line represents the result of a fit of the form $p1 \cdot cos\Phi$ to the data points before deconvolution by the Φ resolution.

The background process for DVCS is a pure QED Bethe-Heitler (BH) where the photon is emitted from the electron. The interference term between DVCS and BH is directly related to GPDs [24]. The beam charge asymmetry is measured by H1 as a function of the azimuthal angle Φ (Fig. 11). For the first time, the interference term is measured via the lepton beam charge asymmetry of the cross sections obtained in a colliding mode, using data recorded in e^+p and e^-p scattering [25]. A significant non zero value is measured.

References

[1] J. Collins, Phys. Rev. D **57** (1998) 3051 [Erratum D **61** (2000) 019902].

[2] A. Aktas et al., H1 Collab., Eur. Phys. J. C **48** (2006) 715, [hep-ex/0606004].

[3] ZEUS Collab., ZEUSprelim-06-024, see www-zeus.desy.de/physics/diff/eps07-pub.html.

[4] ZEUS Collab., ZEUSprelim-06-025, see www-zeus.desy.de/physics/diff/eps07-pub.html.

[5] A. Aktas et al., H1 Collab., Eur. Phys. J. C **49** (2006) 749, [hep-ex/0606003].

[6] S. Chekanov et al., ZEUS Collab., Eur. Phys. J. C **38** (2004) 43.

[7] A. Donnachie and P. V. Landshoff, Nucl. Phys. B **231** (1984) 189.

[8] H1 Collab., H1prelim-06-011,
see www-h1.desy.de/publications/H1preliminary.short-list.html.

[9] G. Ingelman and P. Schlein, Phys. Lett. B **152** (1985) 256.

[10] A. Aktas et al., H1 Collab., Eur. Phys. J. C **50** (2007) 1, [hep-ex/0610076].

[11] A. Aktas et al., H1 Collab., DESY-07-115, [arXiv:0708.3217 hep-ex].

[12] S. Chekanov et al., ZEUS Collab., DESY-07-126.

[13] S. Chekanov et al., ZEUS Collab., Eur. Phys. J. C **51** (2007) 301.

[14] A. Kaidalov et al., Phys. Lett. B **567** (2003) 61.

[15] A. Aktas et al., H1 Collab., Eur. Phys. J. C **51** (2007) 549, [hep-ex/0703022].

[16] S. Chekanov et al., ZEUS Collab., DESY-07-161.

[17] A. Kaidalov et al., [hep-ph/0306134].

[18] H. Abramovicz, L. Frankfurt and M. Strikman, Survey High Energy Phys. **11** (1997) 51.

[19] ZEUS Collab., ZEUSprelim-07-015, see www-zeus.desy.de/physics/diff/eps07-pub.html.

[20] S. Chekanov et al., ZEUS Collab., DESY-07-118.

[21] A. Aktas et al., H1 Collab., DESY-07-142, [arXiv:0709.4114 hep-ex].

[22] ZEUS Collab., ZEUSprelim-07-016, see www-zeus.desy.de/physics/diff/eps07-pub.html.

[23] A. Freud, Phys. Rev. D **68** (2003) 096006, [hep-ph/0306012].

[24] M. Diel, Eur. Phys. J. C **25** (2002) 223, [Erratum C **31** (2003) 277] [hep-ph/0205208].
V. Gurzey and T. Teckentrup, Phys. Rev. D **25** (2006) 054027, [hep-ph/0607099].

[25] H1 Collab., H1prelim-07-011,
see www-h1.desy.de/publications/H1preliminary.short-list.html.

DIFRAKCIJA I TVORBA VEKTORSKIH MEZONA U HERI

Predstavljamo ishode novih mjerenja difrakcijskih udarnih presjeka duboko-nee-lastičnog raspršenja (DIS) i fototvorbe u HERI. Uspoređujemo udarne presjeke tvorbe dvomlazeva i otvorenog šarma s predviđanjima QCD u prvom redu iza vodećeg (NLO), na osnovi funkcija partonske raspodjele dobivenih iz difrakcijskih inkluzivnih DIS podataka. Proveli smo NLO QCD prilagodbu skupno za inkluzivne i DIS podatke radi određivanja difrakcijskih singletnih kvarkovskih i gluonskih gustoća s većom točnošću. Također dajemo pregled nedavnih mjerenja elastične tvorbe vektorskih mezona i duboko virtualnog Comptonovog raspršenja u HERI.